

Exciton crystal melting and destruction by disorder in a bilayer quantum Hall system with a total filling factor of one

Zhengfei Hu  and Kun Yang 

Department of Physics and National High Magnetic Field Laboratory, Florida State University, Tallahassee, Florida 32306, USA



(Received 13 September 2024; revised 10 November 2024; accepted 13 November 2024; published 27 November 2024)

A bilayer quantum Hall system with a total filling factor of one was studied in the regime of a heavy layer imbalance in a recent transport experiment (Y. Zeng *et al.*, [arXiv:2306.16995](https://arxiv.org/abs/2306.16995)), with intriguing new findings. We demonstrate in this paper that (1) the exciton Wigner crystal in this regime can melt into a superfluid phase, giving rise to reentrant superfluid behavior; and (2) in the presence of disorder, electron and hole Wigner crystals in the two layers go through a locking-decoupling transition as the layer separation increases, resulting in a sudden change in the counterflow conductance. A comparison will be made with the findings of the experiments.

DOI: [10.1103/PhysRevB.110.195307](https://doi.org/10.1103/PhysRevB.110.195307)

I. INTRODUCTION

A bilayer quantum Hall system with a total filling factor $\nu_1 + \nu_2 = 1$ has been actively studied for several decades [1–24]. The long-lasting interest in it is due to its extremely rich phase diagram and the fascinating physics associated with the novel phases and transitions among them, which is yet to be exhausted. A recent transport experiment [25] focused on a regime that was underexplored, namely when the two layers are heavily imbalanced, such that $\Delta\nu = \nu_1 - \nu_2 \lesssim 1$, namely $\nu_2 \ll 1$ is the minority layer of electrons, and the hole filling factor in the majority layer 1 is $1 - \nu_1 = \nu_2$. The experiment observed an exciton superfluid-insulator transition predicted more than 20 years ago [10], and revealed some new surprises. The purpose of this paper is to provide theoretical understandings of two of the new findings.

We start by briefly summarizing the relevant observations and basic idea/conclusion of our theoretical work. The experimentalists pass a (drive) current through one of the layers, and measure the current and/or voltage response of the same as well as the opposite layer; the latter corresponds to the drag response [26]. Symmetric and antisymmetric combinations of these responses form normal and counterflow response functions; the latter is usually attributed to the flow of interlayer excitons which are bound pairs of electrons in one layer and holes in the other, assuming they are present and dominate the counterflow transport channel. Bounding between electrons and holes results in the suppression of the free-charge carrier, and hence an insulating state of net in-plane charge transport. The excitons, on the other hand, may either condense to form a superfluid (SF), or crystallize and form an insulating Wigner crystal (WC) state. We will demonstrate that under appropriate conditions an exciton Wigner crystal may melt into a superfluid state, giving rise to reentrant superfluid behavior in the counterflow channel seen in the experiment. We further demonstrate that the presence of an uncorrelated disorder potential in the two layers can disrupt the formation of the interlayer excitons, driving a transition between the exciton Wigner crystal and decoupled electron and hole Wigner

crystals in each layer. This transition manifests itself in some transport anomalies observed in the counterflow channel. It should be noted that there could be other phase transitions, e.g., transitions between the decoupled fractional quantum Hall phase and superfluid at $\Delta\nu = 1/3$ [27]. They will compete with the Wigner crystal phase when $|\Delta\nu|$ moves away from 1.

The rest of the paper is organized as follows. In Sec. II, we calculate the critical temperature of a bilayer exciton superfluid using two previously established effective models [7,10] at a layer imbalance $1 - |\Delta\nu| \ll 1$, and demonstrate it is often higher than the melting temperature of an exciton Wigner crystal. As a result, the crystal melts into a superfluid when this is the case. In Sec. III, we consider the interplay of disorder and interlayer coupling and analyze the competition between them. Clearly, interlayer Coulomb coupling drives the formation of interlayer excitons, while uncorrelated disorder favors the formation of decoupled electron and hole Wigner crystals in each layer. By comparing the energy gains from exciton formation and uncorrelated electron and hole WC distortion in the two layers, we obtain the phase diagram of the system. Some concluding remarks are provided in Sec. IV.

Unless otherwise stated, the magnetic length is assumed to be the length scale, i.e., $l_B = 1$.

II. EXCITON SUPERFLUID AND MELTING OF A WIGNER CRYSTAL

We start by discussing the phases relevant to this section. It is well established that a single-layer two-dimensional (2D) electron gas forms a Wigner crystal at zero temperature for small ν [28–44]. Putting two layers together and holding the total filling factor $\nu_1 + \nu_2 = 1$, the electron (in the minority layer 2) and hole (on the majority layer 1) Wigner crystals with an identical structure lock into an exciton crystal [10], which may melt due to either quantum or thermal fluctuations. Comparisons between the drag current versus drive current, and parallel flow versus counterflow conductance, indicate

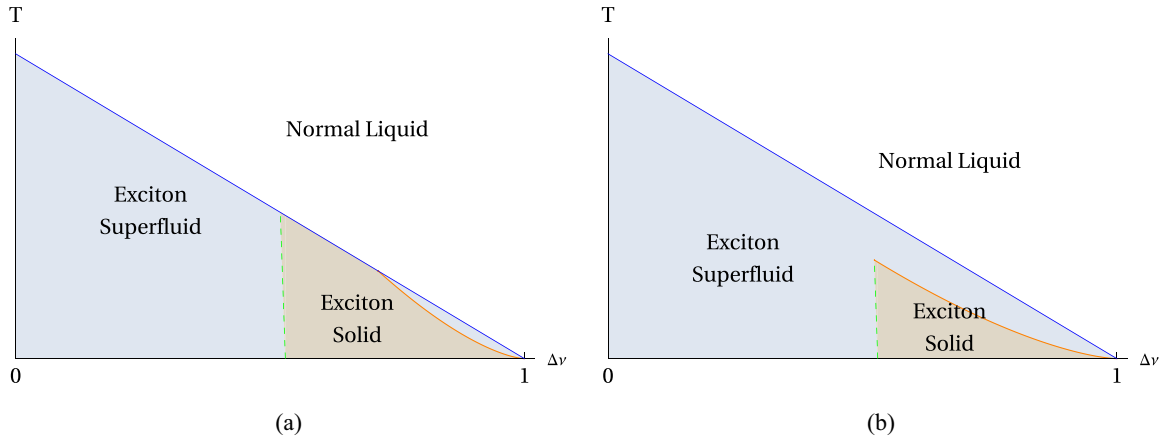


FIG. 1. Finite-temperature phase diagrams near $\Delta\nu = 1$ based on Eqs. (8) and (9). The green dashed line is the natural extension of the zero-temperature phase boundary between the exciton superfluid and Wigner crystal phases. The blue line is the superfluid KT temperature. The orange line is the melting curve of an exciton Wigner crystal. (a) Case with $d > d_c \simeq 2$ in which the exciton Wigner crystal can melt into either a superfluid or normal liquid, depending on $\Delta\nu$. (b) Case with $d < d_c$ where the exciton Wigner crystal can only melt into a superfluid. It should be noted that region far from $\Delta\nu = 1$ shall not be taken too literally.

that the resulting zero-temperature phase is indeed correlated between the two layers [25]. Electrons in one layer and holes in the other tend to bind and condense into an exciton superfluid when d is small and $1 - |\Delta\nu|$ is not too close to 1, and form an exciton Wigner crystal otherwise; see the orange line of Fig. 2 for the schematic zero-temperature phase diagram near $\Delta\nu = 1$. With increasing temperature the exciton Wigner crystal melts into a liquid. We find, surprisingly, that under appropriate conditions the resultant liquid state may be a superfluid.

To understand this we go back to zero temperature, where the exciton superfluid and Wigner crystal phases compete with each other. They are (most likely) separated by a first-order phase boundary, allowing us to consider thermal effects on them at finite temperature separately. As discussed earlier, the exciton Wigner crystal melts into a liquid at some melting temperature which we estimate below. The exciton superfluid, on the other hand, goes through a Kosterlitz-Thouless (KT) transition and becomes a normal fluid. If the superfluid critical (KT) temperature is lower than the melting temperature, we expect WC melts into a normal fluid, which is the usual situation. If it turns out the KT temperature is higher than the melting temperature, we conclude that the WC melts into a superfluid instead, resulting in reentrant superfluidity. The resultant (schematic) phase diagram takes the form of Fig. 1. Our results compare favorably with those of Ref. [25].

To determine the phase diagram we start by calculating the superfluid stiffness which determines the KT temperature of the superfluid phase, and then compare it with the melting temperature of the WC.

A. Phase stiffness and Kosterlitz-Thouless temperature of an exciton superfluid

When $\Delta\nu$ is fixed, the low-temperature superfluid behavior can be described by an effective XY model. In this section we calculate the phase stiffness from two different models: a spin-1/2 easy-plane ferromagnet [7] and a dilute exciton [10]. Once the phase stiffness ρ_s is obtained, the critical

temperature of SF is bounded by $T_c = \frac{\pi\rho_s}{2}$. It turns out in that the vicinity of $\Delta\nu = 1$, the two models lead to the same result. Let $Q^2 = e^2/(4\pi\epsilon)$ for simplicity.

1. Spin-1/2 easy-plane ferromagnet

To begin with, we set up the notations here. Letting $\nu_1 = \nu_\uparrow = 1 - \delta$, $\nu_2 = \nu_\downarrow = \delta$, we have $\Delta\nu = (1 - 2\delta) = \cos\theta = 2(S_\uparrow - S_\downarrow) = m^z$ and $\delta = \frac{1-\Delta\nu}{2} = \sin^2(\theta/2)$, and the density of an electron in one layer

$$n = \delta/2\pi = \sin^2(\theta/2)/2\pi. \quad (1)$$

The gradient energy density of the xy components of local spin is

$$\frac{\rho_E}{2} [(\nabla m^x)^2 + (\nabla m^y)^2], \quad (2)$$

where $\rho_E = -\frac{\nu}{32\pi^2} \int_0^\infty V_k^E h(k) k^3 dk$, and $V_k^E = V_k^A e^{-kd}$, $V_k^A = \frac{2\pi Q^2}{k}$ are Fourier transforms of the intralayer Coulomb potential and interlayer Coulomb potential, respectively [7]. $h(k) = \frac{\nu}{2\pi} \int d^2r (g(r) - 1) \exp(-i\mathbf{k} \cdot \mathbf{r})$ and $g(r) = \langle c^\dagger(\mathbf{r})c(0) \rangle$ are particle-hole correlations of the Laughlin function in momentum space and real space.

For $\nu = 1$, $g(r) = \exp(-r^2)$ and $h(k) = -\exp(-\frac{|k|^2}{2})$, hence we have

$$\rho_E = -\frac{Q^2}{16\pi} \left[d - \sqrt{\frac{\pi}{2}} (d^2 + 1) e^{\frac{d^2}{2}} \operatorname{erfc}(d/\sqrt{2}) \right] \equiv \frac{Q^2 f(d)}{16\pi}, \quad (3)$$

where d is the interlayer spacing, $f(d) = \sqrt{\frac{\pi}{2}} (d^2 + 1) e^{\frac{d^2}{2}} \operatorname{erfc}(d/\sqrt{2}) - d$, and $\operatorname{erfc}(x) = 1 - \operatorname{erf}(x)$ is the complementary error function.

After we obtain ρ_E , the phase stiffness of the XY spin is $\rho_s = \rho_E \sin^2\theta$,

$$\rho_s^{\text{XY}} = \frac{Q^2 f(d)}{4\pi} \frac{\sin^2(\theta)}{4} = \frac{Q^2 f(d)}{8\pi} \frac{1 - (\Delta\nu)^2}{2}, \quad (4)$$

and the critical temperature $T_{\text{KT}} \lesssim \frac{\pi}{2} \rho_s$.

2. Dilute dipolar exciton

From Ref. [10] the inverse effective mass of the exciton is

$$\begin{aligned} m(d)^{-1} &= \frac{Q^2}{2} \int_0^\infty x^2 e^{-xd-x^2/2} dx \\ &= \frac{Q^2}{2} \left(\sqrt{\frac{\pi}{2}} (d^2 + 1) e^{\frac{d^2}{2}} \operatorname{erfc}(d/\sqrt{2}) - d \right) \\ &= \frac{Q^2}{2} f(d). \end{aligned} \quad (5)$$

The boson spectrum given by the Bogoliubov theory (see, e.g., Chap. 18 of Ref. [45]) is

$$E_{\mathbf{k}} = \sqrt{\epsilon_{\mathbf{k}}^2 + 2n\tilde{V}_{q=0}\epsilon_{\mathbf{k}}} \xrightarrow{k \rightarrow 0} \sqrt{2n\tilde{V}_0}\epsilon_{\mathbf{k}} = \hbar v_s k, \quad (6)$$

where the effective interaction $\tilde{V}_k = 2\Delta V_k - \frac{2}{N} \sum_{\mathbf{q}} \Delta V_q e^{-q^2/2}$, $\Delta V = V^A - V^E$ [10]. The Goldstone mode velocity $v_s = \sqrt{\frac{n\tilde{V}_0}{m}}$ is also reported in Ref. [10].

Thereafter the superfluid phase stiffness $\rho_s = \frac{n}{m}$ can be obtained from $n v_s = \rho_s \nabla \theta$ and $\mathbf{v}_s = \nabla \theta / m$ where n is given in (1):

$$\rho_s^{\text{exciton}} = \frac{Q^2 f(d)}{4\pi} \sin^2 \frac{\theta}{2} = \frac{Q^2 f(d)}{8\pi} (1 - \Delta\nu). \quad (7)$$

This expression of superfluid density coincides with the result (4) when $\Delta\nu \rightarrow 1$ (or $\theta \rightarrow 0$) since $\frac{1-(\Delta\nu)^2}{2} = 1 - \Delta\nu - (1 - \Delta\nu)^2/2 \simeq 1 - \Delta\nu$.

We will stick to Eq. (7) and use $T_{\text{KT}} = \pi \rho_s^{\text{exciton}} / 2$ as our estimate of KT temperature,

$$t_{\text{KT}} \equiv T_{\text{KT}} / Q^2 = \frac{f(d)}{16} (1 - \Delta\nu). \quad (8)$$

B. Melting temperature of an exciton Wigner crystal and phase diagrams

In this section we compare the melting temperature of an exciton Wigner crystal, T_m , with the KT temperature estimated above, and determine the finite-temperature phase diagram of the system.

The melting temperature of a classical exciton Wigner crystal was reported to be $T_m \approx 0.0907 \frac{d^2 Q^2}{a^3}$ [46,47]. The relation $a = [\frac{\sqrt{3}}{8\pi} (1 - \Delta\nu)]^{-1/2}$ can be obtained from $\frac{1-\Delta\nu}{2} = \frac{n_e}{1/2\pi}$, where $n_e = 2/(\sqrt{3}a^2)$. We then have dimensionless temperatures

$$t_m = 0.0907 d^2 \left[\frac{\sqrt{3}}{8\pi} (1 - \Delta\nu) \right]^{3/2}, \quad (9)$$

where $t_m = T_m / Q^2$. Comparing Eq. (9) with Eq. (8), we are able to determine the finite-temperature phase diagrams in Fig. 1 for two different situations, both of which are included in the zero-temperature phase diagram in Fig. 2. Two situations are separated by $d_c \simeq 2$. When $d > d_c$, the Wigner crystal could melt into either a superfluid or normal liquid, otherwise it only melts into a superfluid. In the dilute limit $1 - \Delta\nu \ll 1$, the exciton Wigner crystal always melts into a superfluid phase since $t_m < t_{\text{KT}}$ is always true.

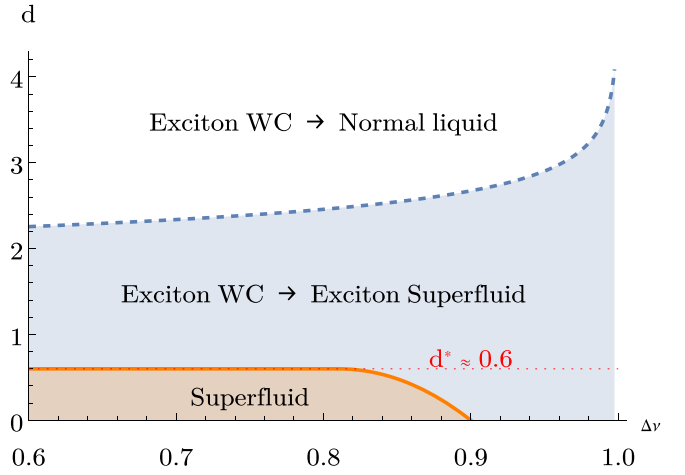


FIG. 2. Schematic zero-temperature phase diagrams near $\Delta\nu = 1$. The orange region denotes the superfluid phase which, due to disorder, terminates before $\Delta\nu = 1$ is reached. The orange solid line is the schematic zero-temperature phase boundary between the superfluid and Wigner crystal. The blue and blank regions are both Wigner crystals at zero temperature, while the blue one melts into a superfluid with increasing temperature and the blank one melts into a normal liquid (see the arrows in the right panel). The blue dashed line is obtained by equating Eq. (9) with Eq. (8). The red dotted line marked by $d^* = 0.6$, reported in Ref. [10], is obtained by comparing the correlation energy per exciton in the superfluid phase and kinetic energy in the crystal phase, above which the superfluid phase is unfavored.

Treating WC as classical leads to an overestimation of T_m , because quantum fluctuation tends to lower T_m as well. Since our goal is to demonstrate the possibility of $T_m < T_{\text{KT}}$, they are justified, and does not change the phase diagram qualitatively. A more serious issue is neglecting the effects of disorder, which are very important when $\Delta\nu \rightarrow 1$, where the excitons are destroyed. This is the focus of the next section. The resultant phase there is a single-layer integer quantum Hall state, which dominates the experimental phase diagram there. One should keep this in mind when comparing with the theoretical phase diagrams in this section obtained *without* taking these into account.

III. LOCKING-DECOUPLING TRANSITION OF A BILAYER WIGNER CRYSTAL

In the previous section we discussed the various phases that can be formed by interlayer excitons, and neglected the effects of disorder. Reference [25] finds a single-layer integer quantum Hall state when $\Delta\nu$ is very close to 1, in which the two layers are essentially decoupled. They also report evidence of a transition into the exciton Wigner crystal phase discussed above. We argue below the existence of the decoupled phase is stabilized by disorder, which also drives the transition. In the absence of a disorder potential, the electron and hole WCs in the two layers always align themselves with each other to minimize the Coulomb energy, resulting in the exciton WC [10]. On the other hand, the disorder potential, which is different in the two layers (assumed to be uncorrelated for simplicity), distorts the two WCs in uncorrelated ways, which

tends to disrupt the formation of excitons and decouples the two layers. By comparing the energy gain and loss between the disorder potential energy and interlayer Coulomb energy, we are able to obtain the transition line for the two layers to become locked/decoupled.

A. Disorder potential energy

We introduce the Gaussian white noise random potential $V_i(\mathbf{r})$ that is uncorrelated between the two layers,

$$\langle V_i(\mathbf{r})V_j(\mathbf{r}') \rangle = \Delta^2 \delta(\mathbf{r} - \mathbf{r}') \delta_{ij}, \quad (10)$$

where $i, j = 1, 2$ are layer indices. The pinning length R of a 2D Wigner crystal, defined as $\langle [u(0) - u(R)]^2 \rangle \simeq a^2$, where a is the lattice constant and $u(R)$ is the field of lattice distortion, is given by balancing the energy gain of the random potential and the energy cost of lattice distortion [48,49]

$$Rn_e \Delta = ca^2, \quad (11)$$

where $n_e = 1/(A_c a^2)$, $A_c = \sqrt{3}/2$ is the density of the electron, and c is the shear modulus. The left- and right-hand sides of this equation stand respectively for the random potential energy gain and elastic energy cost due to the lattice distortion. Since this amount of energy is for a region of linear size R , dividing by R^2 we obtain the density of the random potential energy (for convenience in density comparison we keep one factor of n_e here)

$$\varepsilon_r = \frac{Rn_e \Delta}{R^2} = \frac{n_e \Delta^2}{cA_c a^4}. \quad (12)$$

For a single-layer Wigner crystal of an electron-type interaction and dipole-type interaction we simply take the shear modulus from [50]

$$\begin{aligned} c_1(d \lesssim a) &\approx 2.5 \frac{D^2}{a^5}, & \text{dipole,} \\ c_2 &= 0.3 \frac{Q^2}{a^3}, & \text{charge,} \end{aligned} \quad (13)$$

where $Q^2 = \frac{e^2}{4\pi\epsilon}$, $D^2 = \frac{e^2 d^2}{4\pi\epsilon}$. The transition from a coupled to decoupled picture lowers the disorder potential energy (density) by

$$\Delta\varepsilon_r = \frac{2n_e \Delta^2}{c_1 A_c a^4} - \frac{n_e (\sqrt{2}\Delta)^2}{c_2 A_c a^4} = \frac{2n_e \Delta^2}{A_c a^4} \left(\frac{1}{c_1} - \frac{1}{c_2} \right), \quad (14)$$

where $\sqrt{2}\Delta$ is the effective random potential strength seen by the bilayer [since $V(\mathbf{r}) = V_1(\mathbf{r}) + V_2(\mathbf{r})$ has $\langle V(\mathbf{r})V(\mathbf{r}') \rangle = 2\Delta^2 \delta(\mathbf{r} - \mathbf{r}')$]. On the other hand, in $d \rightarrow \infty$ the interlayer Coulomb energy is diminished and what we have is merely two copies of a single-layer Wigner crystal. Therefore $c_1(\infty) = 2c_2$. In this limit $\Delta\varepsilon_r$ is exactly half of that for individual pinning. In practice, for a specific d in experiments, the effective spacing d/a has an upper bound $d/\sqrt{2}$, which is generally smaller than 1 (see below). For such considerations, we will simply take the dipole approximation $c_1 = 2.5D^2/a^5$.

$$\begin{aligned} \Delta\varepsilon_r &= \frac{2n_e \Delta^2}{A_c Q^2 a} \left(\frac{1}{0.3} - \frac{1}{2.5d^2/a^2} \right) \\ &= q \frac{n_e Q^2}{a} \left(\frac{1}{0.3} - \frac{1}{2.5d^2/a^2} \right), \end{aligned} \quad (15)$$

where

$$q = \frac{2\Delta^2}{A_c Q^4} = \frac{4\Delta^2}{\sqrt{3}Q^4} \quad (16)$$

is the dimensionless random potential strength.

B. Interlayer correlation energy cost

As we demonstrated above, the system can lower the disorder potential energy by distorting the electron and hole WCs in the two layers *independently*, compared to that of the exciton WC. Doing that, however, decouples the two layers and destroys the excitons, resulting in an increase in the interlayer Coulomb interaction energy. In this section we calculate this energy cost.

In this section we let $\frac{Q^2}{a}$ be the energy scale and a , the lattice constant of 2D triangular lattice, be the length scale. We are evaluating the interlayer correlation energy difference of Wigner crystal versus homogeneous electron gas (since the random relative distribution of charges in one layer is seen on average as a homogeneous gas of charge by the other layer), i.e.,

$$\begin{aligned} \Delta E_e &= \int d\mathbf{r} [g_1(\mathbf{r}) - g_2(\mathbf{r})] \frac{-1}{\sqrt{r^2 + d^2}} \\ &= \int d\mathbf{r} \left[\sum_i \delta(\mathbf{r} - \mathbf{R}_i) - 1/A_c \right] \frac{1}{\sqrt{r^2 + d^2}}, \end{aligned} \quad (17)$$

where $g_1(\mathbf{r}) = 1/A_c$, $g_2(\mathbf{r}) = \sum_i \delta(\mathbf{r} - \mathbf{R}_i)$, and $A_c = \sqrt{3}/2$ is the area of unit cell. Compared with Eq. (15), a transition between the locked/decoupled phase will be determined.

In the small d limit, apart from a divergent $1/d$ term, this energy difference is the classic problem of static energy of a 2D Wigner crystal. That is (see, e.g., Refs. [51,52]),

$$\lim_{d \rightarrow 0} [\Delta E_e(d) - 1/d] = -4.213423. \quad (18)$$

We now calculate this energy difference for general d . Let $\Delta E_e = E_0 + E_1 + E_2$, where $E_0 = 1/d$ and

$$\begin{aligned} E_1 &= \frac{1}{\sqrt{\pi}} \left(\int_0^\pi + \int_\pi^\infty \right) dt t^{-1/2} e^{-td} \sum' e^{-tR_i^2} \equiv E_{11} + E_{12}, \\ E_2 &= -\frac{1}{A_c} \int d\mathbf{r} \frac{e^2}{\sqrt{r^2 + d^2}} \\ &= -\frac{1}{\sqrt{\pi} A_c} \int_0^\infty dt \int d\mathbf{r} e^{-tr^2} e^{-td^2} t^{-1/2} \\ &= -\frac{\sqrt{\pi}}{A_c} \int_0^\infty dt t^{-3/2} e^{-td^2} \\ &= -\frac{\sqrt{\pi}}{A_c} \int_0^\pi dt t^{-3/2} e^{-td^2} - \frac{2}{A_c} [e^{-\pi d^2} - \pi d \operatorname{erfc}(\sqrt{\pi} d)], \end{aligned} \quad (19)$$

where $\Gamma(n)z^{-n} = \int_0^\infty t^{n-1} e^{-zt} dt$ is used in rewriting $1/\sqrt{d^2 + r^2} = \frac{1}{\sqrt{\pi}} \int_0^\infty t^{-1/2} e^{-t(d^2+r^2)} dt$, and $\sqrt{\pi} \int_\pi^\infty dt t^{-3/2} e^{-td^2} = \frac{2}{\sqrt{\pi}} [e^{-\pi d^2} - \pi d \operatorname{erfc}(\sqrt{\pi} d)]$. \sum' stands for the summation excluding $R_i = 0$.

Letting $t = \pi x$, we have

$$E_{12} = \int_1^\infty dx x^{-1/2} \sum' e^{-\pi x(d^2 + R_i^2)} = \sum' \operatorname{erfc} \left[\sqrt{\pi(d^2 + R_i^2)} \right] / \sqrt{(d^2 + R_i^2)}, \quad (20)$$

where $\int_1^\infty x^{-1/2} e^{-\pi x a^2} dx = \operatorname{erfc}(\sqrt{\pi} a)/a$ is utilized. To calculate E_{11} we first complete it with an $R_i = 0$ term,

$$\begin{aligned} E_{11} &= \frac{1}{\sqrt{\pi}} \int_0^\pi dt t^{-1/2} e^{-td^2} \Theta_\Gamma(t/\pi) - \frac{1}{\sqrt{\pi}} \int_0^\pi t^{-1/2} e^{-td^2} dt = \frac{\sqrt{\pi}}{A_c} \int_0^\pi dt t^{-3/2} e^{-td^2} \Theta_{\Gamma'}(\pi/t) - \operatorname{erf}(\sqrt{\pi} d)/d \\ &= \frac{1}{A_c} \int_1^\infty dx x^{-1/2} e^{-\pi d^2/x} \sum' e^{-\pi x K_i^2} - \operatorname{erf}(\sqrt{\pi} d)/d + \frac{\sqrt{\pi}}{A_c} \int_0^\pi dt t^{-3/2} e^{-td^2}, \end{aligned} \quad (21)$$

with $\Theta_\Gamma(t) \equiv \sum_{\mathbf{R}_i \in \Gamma} e^{-\pi t R_i^2}$, Γ being a lattice. From the first line to the second line we used $\int_0^1 t^{-1/2} e^{-\pi t d^2} dt = \operatorname{erf}(a\sqrt{\pi})/a$ and $\Theta_\Gamma(t) = t^{-n/2} v(\Gamma)^{-1} \Theta_{\Gamma'}(1/t)$, where Γ' is the dual of lattice Γ , $v(\Gamma)$ is the measure of the unit cell of Γ , and n is the dimension of the lattice Γ (see, e.g., p. 115 of Ref. [53]); from the second line to the third line, points of the dual lattice are denoted as \mathbf{K}_i and we let $t = \pi/x$ for all $K_i \equiv |\mathbf{K}_i| \neq 0$ terms. Note that the very last divergent term in E_{11} cancels the divergent part of E_2 .

Since

$$\int_1^\infty dx x^{-1/2} e^{-\pi(d^2/x + K_i^2 x)} = \frac{e^{-2\pi d K_i} \{1 + \operatorname{erf}[\sqrt{\pi}(d - K_i)]\} + e^{2\pi d K_i} \{1 - \operatorname{erf}[\sqrt{\pi}(d + K_i)]\}}{2K_i} \equiv \phi_{-1/2}(d, K_i), \quad (22)$$

we have

$$E_1 + E_2 = -\frac{\operatorname{erf}(\sqrt{\pi} d)}{d} - \frac{2}{A_c} [e^{-\pi d^2} - \pi d \operatorname{erfc}(\sqrt{\pi} d)] + \sum' \frac{\operatorname{erfc} \left[\sqrt{\pi(d^2 + R_i^2)} \right]}{\sqrt{d^2 + R_i^2}} + \frac{1}{A_c} \sum' \phi_{-1/2}(d, K_i). \quad (23)$$

For a sanity check, letting $d \rightarrow 0$ we have

$$\begin{aligned} E_1 + E_2 &= -2 \left(1 + \frac{1}{A_c} \right) + \sum' \operatorname{erfc}(\sqrt{\pi} R_i)/R_i + \frac{1}{A_c} \sum' \operatorname{erfc}(\sqrt{\pi} K_i)/K_i \\ &\cong -2 \left(1 + \frac{1}{A_c} \right) + 6 \operatorname{erfc}(\sqrt{\pi}) + 6 \operatorname{erfc}(\sqrt{\pi}/A_c) = -4.213475, \end{aligned} \quad (24)$$

where we took the nearest lattice point approximation, i.e., only six terms with the smallest R_i, K_i in the those lattice summations are kept. Nevertheless, the result matches the known static energy for a 2D Wigner crystal up to the fourth digit.

For general d , let $\delta E(d)$ be the nearest lattice point approximation of $E_1 + E_2$ in Eq. (23),

$$\begin{aligned} \delta E(d) &= -\frac{\operatorname{erf}(\sqrt{\pi} d)}{d} - \frac{2[e^{-\pi d^2} - \pi d \operatorname{erfc}(\sqrt{\pi} d)]}{A_c} + \frac{6 \operatorname{erfc} \left[\sqrt{\pi(d^2 + 1)} \right]}{\sqrt{d^2 + 1}} \\ &\quad + 3 \left\{ e^{-2\pi d/A_c} \left(1 + \operatorname{erf} \left[\sqrt{\pi} \left(d - \frac{1}{A_c} \right) \right] \right) + e^{2\pi d/A_c} \operatorname{erfc} \left[\sqrt{\pi} \left(d + \frac{1}{A_c} \right) \right] \right\}, \end{aligned} \quad (25)$$

$1/A_c = 2/\sqrt{3}$ comes from the lattice constant of the dual lattice. It behaves asymptotically in the $d \rightarrow \infty$ limit as $\delta E(d) + 1/d \sim 6e^{-4\pi d/\sqrt{3}}$. Also for $d \rightarrow \infty$, $\operatorname{erfc}[\sqrt{\pi(d^2 + R_i^2)}]/\sqrt{d^2 + R_i^2} \sim e^{-\pi(d^2 + R_i^2)}/[\pi(d^2 + R_i^2)]$ and $\operatorname{erfc}(\sqrt{\pi} x) \sim e^{-\pi x^2}/(\pi x)$ results in

$$\phi_{-1/2}(d, K_i) \leq \{2e^{-2\pi d K_i} + e^{-\pi(d^2 + K_i^2)}/[\pi(d + K_i)]\}/(2K_i). \quad (26)$$

All terms generated from farther lattice points are dominated by $6e^{-4\pi d/\sqrt{3}}$. In the sense that $\delta E(d)$ is a good approximation to $E_1 + E_2$ for both $d \rightarrow 0$ and $d \rightarrow \infty$, we could safely take

$$\Delta E_e \cong 1/d + \delta E(d). \quad (27)$$

Putting back dimensions, the Coulomb energy density difference is, with δE defined in Eq. (25),

$$\Delta \varepsilon_e \cong n_e \frac{Q^2}{a} [a/d + \delta E(d/a)]. \quad (28)$$

C. Phase diagram

Comparing (15) with (28) we can immediately see that the transition between coupled/decoupled phases is determined by the root of the dimensionless equation

$$\begin{aligned} \frac{q}{0.3} x^2 - x - q/2.5 - x^2 \delta E(x) &= 0, \\ x = d/a &= d \sqrt{\frac{\sqrt{3}}{8\pi} (1 - \Delta v)}, \end{aligned} \quad (29)$$

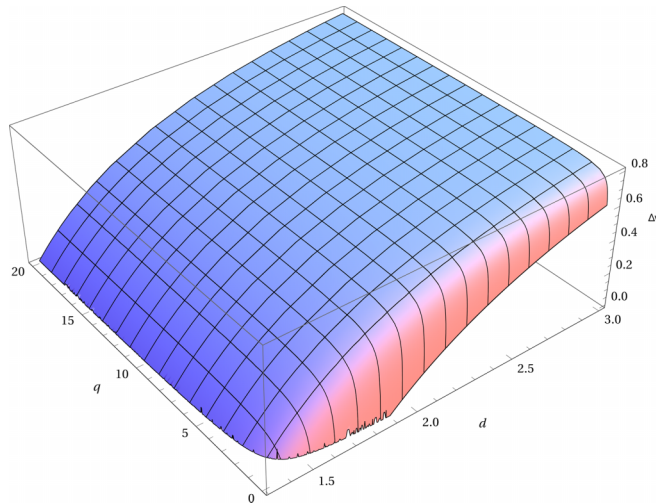


FIG. 3. Phase diagram of the coupled/decoupled Wigner crystal plotted from Eq. (29). $q = \frac{4\Delta^2}{\sqrt{3}Q^4}$ characterizes the random potential strength, where Δ is defined in Eq. (10) and $Q^2 = e^2/(4\pi\epsilon)$. The region under the surface is a decoupled electron-hole Wigner crystal while the region above it is an exciton Wigner crystal.

where q , defined in Eq. (16), is, up to a constant, the energy scale of the random potential comparing with the Coulomb energy. Putting together, we can draw a phase diagram in Fig. 3 for the decoupled electron-hole Wigner crystal and exciton Wigner crystal.

IV. CONCLUDING REMARKS

In this paper, we analyzed the competition between different phases in a bilayer quantum Hall system with a total filling factor of one driven by temperature and/or disorder. Our results compare favorably with a recent experiment [25]. Particularly interesting (and surprising) among our findings is that the exciton superfluid can (often) result from melting an exciton WC. This bears a remarkable similarity to the observation [54] that the melting of electron WC at a low filling factor results in fractional quantum Hall liquids. Similar phenomena were observed very recently in systems supporting (fractional) anomalous quantum Hall states [55]. We speculate that the melting of electron or hole WC in these systems resulted in the formation of fractional anomalous quantum Hall states. We also note that it is in principle possible to have the WC and SF orders coexist, resulting in an exciton supersolid. It is a very interesting future direction of research to look for such a novel phase, both experimentally and theoretically.

ACKNOWLEDGMENTS

We thank Cory Dean, Lloyd Engel, and Leo Li for helpful discussions. This work was supported by the National Science Foundation Grant No. DMR-2315954, and performed at the National High Magnetic Field Laboratory which is supported by National Science Foundation Cooperative Agreement No. DMR-2128556, and the State of Florida.

-
- [1] X.-G. Wen and A. Zee, Neutral superfluid modes and “magnetic” monopoles in multilayered quantum Hall systems, *Phys. Rev. Lett.* **69**, 1811 (1992).
 - [2] Z. F. Ezawa and A. Iwazaki, Chern-Simons gauge theory for double-layer electron system, *Int. J. Mod. Phys. B* **06**, 3205 (1992).
 - [3] J. P. Eisenstein, G. S. Boebinger, L. N. Pfeiffer, K. W. West, and S. He, New fractional quantum Hall state in double-layer two-dimensional electron systems, *Phys. Rev. Lett.* **68**, 1383 (1992).
 - [4] X. G. Wen and A. Zee, Tunneling in double-layered quantum Hall systems, *Phys. Rev. B* **47**, 2265 (1993).
 - [5] K. Yang, K. Moon, L. Zheng, A. H. MacDonald, S. M. Girvin, D. Yoshioka, and S.-C. Zhang, Quantum ferromagnetism and phase transitions in double-layer quantum Hall systems, *Phys. Rev. Lett.* **72**, 732 (1994).
 - [6] L. V. Butov, A. Zrenner, G. Abstreiter, G. Böhm, and G. Weimann, Condensation of indirect excitons in coupled AlAs/GaAs quantum wells, *Phys. Rev. Lett.* **73**, 304 (1994).
 - [7] K. Moon, H. Mori, K. Yang, S. M. Girvin, A. H. MacDonald, L. Zheng, D. Yoshioka, and S.-C. Zhang, Spontaneous interlayer coherence in double-layer quantum Hall systems: Charged vortices and Kosterlitz-Thouless phase transitions, *Phys. Rev. B* **51**, 5138 (1995).
 - [8] K. Yang, K. Moon, L. Belkhir, H. Mori, S. M. Girvin, A. H. MacDonald, L. Zheng, and D. Yoshioka, Spontaneous interlayer coherence in double-layer quantum Hall systems: Symmetry-breaking interactions, in-plane fields, and phase solitons, *Phys. Rev. B* **54**, 11644 (1996).
 - [9] M. P. Lilly, J. P. Eisenstein, L. N. Pfeiffer, and K. W. West, Coulomb drag in the extreme quantum limit, *Phys. Rev. Lett.* **80**, 1714 (1998).
 - [10] K. Yang, Dipolar excitons, spontaneous phase coherence, and superfluid-insulator transition in bilayer quantum Hall systems at $\nu = 1$, *Phys. Rev. Lett.* **87**, 056802 (2001).
 - [11] L. V. Butov, A. C. Gossard, and D. S. Chemla, Macroscopically ordered state in an exciton system, *Nature (London)* **418**, 751 (2002).
 - [12] J. P. Eisenstein and A. H. MacDonald, Bose-Einstein condensation of excitons in bilayer electron systems, *Nature (London)* **432**, 691 (2004).
 - [13] M. Kellogg, J. P. Eisenstein, L. N. Pfeiffer, and K. W. West, Vanishing Hall resistance at high magnetic field in a double-layer two-dimensional electron system, *Phys. Rev. Lett.* **93**, 036801 (2004).
 - [14] E. Tutuc, M. Shayegan, and D. A. Huse, Counterflow measurements in strongly correlated GaAs hole bilayers: Evidence for electron-hole pairing, *Phys. Rev. Lett.* **93**, 036802 (2004).
 - [15] R. D. Wiersma, J. G. S. Lok, S. Kraus, W. Dietsche, K. von Klitzing, D. Schuh, M. Bichler, H.-P. Tranitz, and W. Wegscheider, Activated transport in the separate layers that form the $\nu_l = 1$ exciton condensate, *Phys. Rev. Lett.* **93**, 266805 (2004).
 - [16] B. Seradjeh, H. Weber, and M. Franz, Vortices, zero modes, and fractionalization in the bilayer-graphene exciton condensate, *Phys. Rev. Lett.* **101**, 246404 (2008).

- [17] L. Tiemann, J. G. S. Lok, W. Dietsche, K. von Klitzing, K. Muraki, D. Schuh, and W. Wegscheider, Exciton condensate at a total filling factor of one in Corbino two-dimensional electron bilayers, *Phys. Rev. B* **77**, 033306 (2008).
- [18] R. T. Weitz, M. T. Allen, B. E. Feldman, J. Martin, and A. Yacoby, Broken-symmetry states in doubly gated suspended bilayer graphene, *Science* **330**, 812 (2010).
- [19] Y. Barlas, K. Yang, and A. H. MacDonald, Quantum Hall effects in graphene-based two-dimensional electron systems, *Nanotechnology* **23**, 052001 (2012).
- [20] D. Nandi, A. D. K. Finck, J. P. Eisenstein, L. N. Pfeiffer, and K. W. West, Exciton condensation and perfect Coulomb drag, *Nature (London)* **488**, 481 (2012).
- [21] J. Eisenstein, Exciton condensation in bilayer quantum Hall systems, *Annu. Rev. Condens. Matter Phys.* **5**, 159 (2014).
- [22] X. Liu, K. Watanabe, T. Taniguchi, B. I. Halperin, and P. Kim, Quantum Hall drag of exciton condensate in graphene, *Nat. Phys.* **13**, 746 (2017).
- [23] J. I. A. Li, T. Taniguchi, K. Watanabe, J. Hone, and C. R. Dean, Excitonic superfluid phase in double bilayer graphene, *Nat. Phys.* **13**, 751 (2017).
- [24] G. W. Burg, N. Prasad, K. Kim, T. Taniguchi, K. Watanabe, A. H. MacDonald, L. F. Register, and E. Tutuc, Strongly enhanced tunneling at total charge neutrality in double-bilayer graphene-WSe₂ heterostructures, *Phys. Rev. Lett.* **120**, 177702 (2018).
- [25] Y. Zeng, Q. Shi, A. Okounkova, D. Sun, K. Watanabe, T. Taniguchi, J. Hone, C. R. Dean, and J. I. A. Li, Evidence for a superfluid-to-solid transition of bilayer excitons, [arXiv:2306.16995](https://arxiv.org/abs/2306.16995).
- [26] T. J. Gramila, J. P. Eisenstein, A. H. MacDonald, L. N. Pfeiffer, and K. W. West, Mutual friction between parallel two-dimensional electron systems, *Phys. Rev. Lett.* **66**, 1216 (1991).
- [27] H. Chen and K. Yang, Interaction-driven quantum phase transitions in fractional topological insulators, *Phys. Rev. B* **85**, 195113 (2012).
- [28] E. Wigner, On the interaction of electrons in metals, *Phys. Rev.* **46**, 1002 (1934).
- [29] K. Maki and X. Zotos, Static and dynamic properties of a two-dimensional Wigner crystal in a strong magnetic field, *Phys. Rev. B* **28**, 4349 (1983).
- [30] D. Yoshioka and P. A. Lee, Ground-state energy of a two-dimensional charge-density-wave state in a strong magnetic field, *Phys. Rev. B* **27**, 4986 (1983).
- [31] P. K. Lam and S. M. Girvin, Liquid-solid transition and the fractional quantum-Hall effect, *Phys. Rev. B* **30**, 473 (1984).
- [32] A. H. MacDonald and G. W. Bryant, Strong-magnetic-field states of the pure electron plasma, *Phys. Rev. Lett.* **58**, 515 (1987).
- [33] V. J. Goldman, M. Santos, M. Shayegan, and J. E. Cunningham, Evidence for two-dimensional quantum Wigner crystal, *Phys. Rev. Lett.* **65**, 2189 (1990).
- [34] G. Senatore and N. H. March, Recent progress in the field of electron correlation, *Rev. Mod. Phys.* **66**, 445 (1994).
- [35] H. C. Manoharan and M. Shayegan, Wigner crystal versus Hall insulator, *Phys. Rev. B* **50**, 17662 (1994).
- [36] M. Shayegan, Case for the magnetic-field-induced two-dimensional Wigner crystal, in *Perspectives in Quantum Hall Effects*, edited by S. Das Sarma and A. Pinczuk (Wiley, Hoboken, NJ, 1996), Chap. 9.
- [37] R. K. Kamilla and J. K. Jain, Excitonic instability and termination of fractional quantum Hall effect, *Phys. Rev. B* **55**, R13417(R) (1997).
- [38] K. Yang, F. D. M. Haldane, and E. H. Rezayi, Wigner crystals in the lowest Landau level at low-filling factors, *Phys. Rev. B* **64**, 081301(R) (2001).
- [39] P. D. Ye, L. W. Engel, D. C. Tsui, R. M. Lewis, L. N. Pfeiffer, and K. West, Correlation lengths of the Wigner-crystal order in a two-dimensional electron system at high magnetic fields, *Phys. Rev. Lett.* **89**, 176802 (2002).
- [40] Y. P. Chen, G. Sambandamurthy, Z. H. Wang, R. M. Lewis, L. W. Engel, D. C. Tsui, P. D. Ye, L. N. Pfeiffer, and K. W. West, Melting of a 2D quantum electron solid in high magnetic field, *Nat. Phys.* **2**, 452 (2006).
- [41] P. Monceau, Electronic crystals: An experimental overview, *Adv. Phys.* **61**, 325 (2012).
- [42] H. Deng, L. N. Pfeiffer, K. W. West, K. W. Baldwin, L. W. Engel, and M. Shayegan, Probing the melting of a two-dimensional quantum Wigner crystal via its screening efficiency, *Phys. Rev. Lett.* **122**, 116601 (2019).
- [43] T. Smoleński, P. E. Dolgirev, C. Kuhlenkamp, A. Popert, Y. Shimazaki, P. Back, X. Lu, M. Kroner, K. Watanabe, T. Taniguchi, I. Esterlis, E. Demler, and A. Imamoğlu, Signatures of Wigner crystal of electrons in a monolayer semiconductor, *Nature (London)* **595**, 53 (2021).
- [44] Y.-C. Tsui, M. He, Y. Hu, E. Lake, T. Wang, K. Watanabe, T. Taniguchi, M. P. Zaletel, and A. Yazdani, Direct observation of a magnetic-field-induced Wigner crystal, *Nature (London)* **628**, 287 (2024).
- [45] S. M. Girvin and K. Yang, *Modern Condensed Matter Physics* (Cambridge University Press, Cambridge, U.K., 2019).
- [46] H. H. von Grünberg, P. Keim, K. Zahn, and G. Maret, Elastic behavior of a two-dimensional crystal near melting, *Phys. Rev. Lett.* **93**, 255703 (2004).
- [47] R. K. Kalia and P. Vashishta, Interfacial colloidal crystals and melting transition, *J. Phys. C: Solid State Phys.* **14**, L643 (1981).
- [48] R. Chitra, T. Giamarchi, and P. Le Doussal, Pinned Wigner crystals, *Phys. Rev. B* **65**, 035312 (2001).
- [49] M. M. Fogler and D. A. Huse, Dynamical response of a pinned two-dimensional Wigner crystal, *Phys. Rev. B* **62**, 7553 (2000).
- [50] G. M. Bruun and D. R. Nelson, Quantum hexatic order in two-dimensional dipolar and charged fluids, *Phys. Rev. B* **89**, 094112 (2014).
- [51] L. Bonsall and A. A. Maradudin, Some static and dynamical properties of a two-dimensional Wigner crystal, *Phys. Rev. B* **15**, 1959 (1977).
- [52] D. Borwein, J. M. Borwein, R. Shail, and I. J. Zucker, Energy of static electron lattices, *J. Phys. A: Math. Gen.* **21**, 1519 (1988).
- [53] J.-P. Serre, *A Course in Arithmetic* (Springer, New York, 1973).
- [54] W. Pan, H. L. Stormer, D. C. Tsui, L. N. Pfeiffer, K. W. Baldwin, and K. W. West, Transition from an electron solid to the sequence of fractional quantum Hall states at very low Landau level filling factor, *Phys. Rev. Lett.* **88**, 176802 (2002).
- [55] Z. Lu, T. Han, Y. Yao, J. Yang, J. Seo, L. Shi, S. Ye, K. Watanabe, T. Taniguchi, and L. Ju, Extended quantum anomalous Hall states in graphene/hBN moiré superlattices, [arXiv:2408.10203](https://arxiv.org/abs/2408.10203).